

EUROPEAN ORGANIZATION FOR NUCLEAR RESEARCH

ALEPH 2001-066 CONF 2001-046
DELPHI 2001-113 CONF 536
L3 Note 2699
OPAL Physics Note PN479
LHWG Note/2001-03
CERN-EP/2001-xxx
October 27, 2018

Search for the Standard Model Higgs Boson at LEP

ALEPH, DELPHI, L3 and OPAL Collaborations

The LEP working group for Higgs boson searches

Abstract

The four LEP collaborations, ALEPH, DELPHI, L3 and OPAL, have collected 2465 pb^{-1} of e^+e^- collision data at energies between 189 and 209 GeV, of which 542 pb^{-1} were collected above 206 GeV. Searches for the Standard Model Higgs boson have been performed by each of the LEP collaborations. Their data have been combined and examined for their consistency with the Standard Model background and various Standard Model Higgs boson mass hypotheses. A lower bound of 114.1 GeV has been obtained at the 95% confidence level for the mass of the Higgs boson. The likelihood analysis shows a preference for a Higgs boson with a mass of 115.6 GeV. At this mass, the probability for the background to generate the observed effect is 3.4%.

THE RESULTS QUOTED IN THIS PAPER ARE NOT FINAL

1 Introduction

The Higgs mechanism [1] plays a central role in the unification of the electromagnetic and weak interactions by providing mass to the intermediate vector bosons, W and Z, without violating local gauge invariance. Within the Standard Model (SM) [2], the Higgs mechanism predicts a single neutral scalar particle, the Higgs boson. Its mass is arbitrary; however, self-consistency of the model up to a scale Λ imposes an upper [3] and lower bound [4]. If Λ is close to the Planck scale, the mass of the SM Higgs boson is confined between about 130 and 190 GeV [5]. A mass less than 130 GeV would indicate physics beyond the SM to set in below the Planck scale; for example, in the minimal supersymmetric extension of the SM the mass of the lightest neutral scalar h^0 is predicted to be less than 135 GeV [6]. Even stronger bounds are obtained using arguments of naturalness and fine-tuning [7].

Indirect experimental constraints are derived from precision measurements of electroweak parameters which depend in their interpretation on the log of the Higgs boson mass via radiative corrections. If the SM is assumed, the currently preferred mass value is $m_H = 88^{+53}_{-33}$ GeV, and the 95% confidence level upper bound on the mass is 196 GeV [8].

Direct searches carried out by the four LEP collaborations in data collected prior to the year 2000 did not reveal any signal for the SM Higgs boson. When the LEP data were statistically added, the observed event rate and their distributions have shown good agreement with the SM background processes [9, 10, 11].

The situation changed during summer 2000 with the advent of new LEP data, at centre-of-mass energies exceeding 206 GeV. At the session of the LEP Committee of September 5, 2000, ALEPH reported an excess of events suggesting the production of a SM Higgs boson with mass in the vicinity of 115 GeV [12] while DELPHI, L3 and OPAL did not support this observation. The quoted probabilities for the SM background to produce the observed event configuration ($1 - CL_b$, as defined below in Section 2.5), are listed in the first line of Table 1 where the LEP combined result is also quoted. Due to this ambiguous situation, the LEP shutdown planned for the end of September was postponed by one month, and all effort was made to maximize the LEP energy.

	ALEPH	DELPHI	L3	OPAL	LEP
LEPC, Sept 5 (*)	1.6×10^{-4}	0.67	0.84	0.47	2.5×10^{-2}
LEPC, Nov 3 [13]	6.5×10^{-4}	0.68	0.068	0.19	4.2×10^{-3}
Ref's [15, 16, 17, 18]	2.6×10^{-3}	0.77	0.32	0.20	

Table 1: Background probabilities ($1 - CL_b$) at a Higgs boson test-mass of $m_H = 115$ GeV, for the individual experiments and for the LEP data combined. (*) The results presented at the Sept. 5 LEPC have been revised for the LEPC of Nov. 3. The values listed are the revised ones [13].

A rapid analysis which included the bulk part of the new data resulted in the probabilities

listed in the second line of Table 1. These results were presented at the LEP Committee meeting of November 3, 2000 [13]. The ALEPH excess was slightly attenuated, as indicated by the increased background probability. On the other hand, L3 reported some candidates suggesting the Higgs boson interpretation [14].

After a thorough review of the analysis procedures, the LEP collaborations have published their results [15, 16, 17, 18], updating them to include all data. The L3 publication [17] is final. The review addressed many potential systematic errors, especially in the handling of a signal at the kinematic limit of the production process $e^+e^- \rightarrow ZH$. Also, the uncertainties from Monte Carlo statistics were reduced and in some cases the search sensitivity has been improved. The published background probabilities at a test-mass of 115 GeV are reported in the last line of Table 1. The ALEPH [15] and L3 [17] excesses have decreased since the beginning of November.

In this paper we present combined results from LEP which are based on these recent publications. However, the inputs also include data collected before the year 2000. The c.m. energies (E_{cm}) thus span the range from 189 GeV to 209 GeV. The integrated luminosities by experiment and energy are given in Table 2.

	ALEPH	DELPHI	L3	OPAL	LEP
$E_{cm} \geq 189$ GeV	629	610	627	599	2465
$E_{cm} \geq 206$ GeV	130	142	139	130	542

Table 2: Integrated luminosities (pb^{-1}) of the data samples provided by the four experiments for the present combination, and of the total LEP sample. Subsets taken at energies larger than 206 GeV are listed separately.

At LEP energies, the SM Higgs boson is expected to be produced mainly in association with a Z boson through the Higgsstrahlung process, $e^+e^- \rightarrow HZ$ [19]. Small additional contributions are expected from t-channel W and Z boson fusion processes, which produce a Higgs boson and either a pair of neutrinos or electrons in the final state [20]. For masses in the vicinity of 115 GeV (the kinematic limit for Higgsstrahlung at $E_{cm} \approx 206$ GeV), the SM Higgs boson is expected to decay mainly into $b\bar{b}$ quark pairs (74%) while decays to tau lepton pairs, WW^* , gluon pairs ($\approx 7\%$ each), and to $c\bar{c}$ ($\approx 4\%$) are all less important. The final-state topologies are determined by these decays and by the decay of the associated Z boson. The searches at LEP encompass the four-jet final state ($H \rightarrow b\bar{b}$) $q\bar{q}$, the missing energy final state ($H \rightarrow b\bar{b}$) $\nu\bar{\nu}$, the leptonic final state ($H \rightarrow b\bar{b}$) $\ell^+\ell^-$ where ℓ denotes an electron or a muon, and the tau lepton final states ($H \rightarrow b\bar{b}$) $\tau^+\tau^-$ and ($H \rightarrow \tau^+\tau^-$) $(Z \rightarrow q\bar{q})$.

Preselection cuts are applied to reduce the main background from two-photon processes and from radiative returns to the Z boson, $e^+e^- \rightarrow Z\gamma(\gamma)$. The remaining background, mainly from fermion pairs (possibly with photon or gluon radiation), WW , and ZZ , is reduced by applying cuts which make use of kinematic differences between the signal and the background processes and of the requirement of b-flavour, abundant in the decay of the Higgs boson. The detailed implementation of these selections and analysis procedures is different for each experiment [15]-

[18]. In some search channels ¹, the selection depends explicitly upon the hypothesized Higgs boson mass.

2 Combination procedure and results

2.1 Input provided by the experiments

The information provided by the LEP experiments as input to the combination is in most cases binned in two discriminating variables: (i) the reconstructed Higgs boson mass m_H^{rec} , and (ii) a variable \mathcal{G} which combines many features of the events and allows the analysis to distinguish on a statistical basis between events from the Higgs boson signal and events from background processes. This variable is typically the outcome of a likelihood analysis or the output of an artificial neural network. Variables which tag b-flavoured jets contribute in an essential way to the value of \mathcal{G} .

In a given bin i of the plane defined by m_H^{rec} and \mathcal{G} , the experiments provide the number N_i of selected data events, the expected background rate b_i , and the expected signal $s_i(m_H)$ for a set of hypothesized Higgs boson masses (test-mass m_H hereafter). In those channels where the selection depends on m_H , the values of N_i and b_i are also given for a set of m_H values. For a given test-mass, a weight of s/b can thus be assigned to each selected candidate, depending on m_H and the bin where it is reconstructed. The estimation of s_i and b_i makes use of detailed Monte Carlo simulations which take into account all known experimental features such as the c.m. energy and integrated luminosity of the data samples, cross-sections and decay branching ratios for the signal and background processes, selection efficiencies, experimental resolutions with non-gaussian contributions and systematic errors with their correlations. Since the simulation is done at fixed sets of E_{cm} and m_H , interpolation procedures such as [21] are applied to obtain the distributions which correspond to arbitrary energies and test-masses. In order to avoid problems which might arise in some bins due to low Monte Carlo statistics, smoothing procedures such as [22] are applied which use the corresponding information in the neighbouring bins.

2.2 Hypothesis testing

The observed data configuration in the $[m_H^{rec}, \mathcal{G}]$ plane is subjected to a likelihood test of two hypothetical scenarios. In the background scenario it is assumed that the data receive contributions from the SM background processes only while in the signal+background scenario the contribution from a Higgs boson of test-mass m_H is assumed in addition. The expressions

¹In the following, the word channel designates any subset of the data where the Higgs boson search is carried out; these may correspond to different final state topologies, to subsets of data collected at different c.m. energies or to subsets provided by different experiments.

for the corresponding likelihoods, \mathcal{L}_b and \mathcal{L}_{s+b} , are given e.g. in Appendix A of Ref. [9]. The ratio

$$Q = \mathcal{L}_{s+b}/\mathcal{L}_b \quad (1)$$

serves as test-statistic allowing to rank any data configuration between the background and signal+background hypotheses. For convenience, the quantity

$$-2 \ln Q = 2s_{tot} - 2 \sum_i N_i \ln[1 + s_i/b_i] \quad (2)$$

is used since in the limit of high statistics it corresponds to the difference in χ^2 between the two hypotheses. In the above expression, $s_{tot} = \sum_i s_i$ is the total expected signal rate. This test-statistic has been adopted since it makes the most efficient use of the information available in the observed event configuration of a search, similarly to the way the principle of maximum likelihood gives the most efficient estimators of parameters in a measurement.

Figure 1 shows the test-statistic $-2 \ln Q$ as a function of the test-mass for the present combination of LEP data. The expected curves and their spreads are obtained by replacing the observed data configuration by a large number of simulated event configurations.

There is a minimum in the observed $-2 \ln Q$ at $m_H = 115.6$ GeV (maximum of the likelihood ratio Q) indicating a deviation from the background hypothesis. The minimum coincides with the signal+background expectation for the same test-mass. The value of $-2 \ln Q$ at $m_H = 115.6$ GeV is -2.88 .

Another feature in Figure 1 is a persistent tail in the observation towards lower test-masses where the observed curve stays away from the prediction for background. This is interpreted as being due to a large extent to the experimental resolution. A test has been performed where the signal expected from a 115 GeV Higgs boson was injected in the background simulation and propagated through the likelihood ratio calculation at each m_H value. Although the resulting curve (dotted line) reproduces the main feature of the observed tail², local excess events due to statistical fluctuations can also contribute to the tail.

In Figures 2 and 3 the likelihood test is applied to subsets of the data, from individual experiments and final-state topologies. In the vicinity of $m_H = 115$ GeV, the signal-like behaviour mainly originates from the ALEPH data and is concentrated in the four-jet final state. One should note that none of the four experiments, taken separately, have the statistical power to distinguish between the background and the signal+background hypotheses at the level of two standard deviations for a test mass of 115 GeV (see the intersection of the signal+background curve with the lower edge of the light-shaded bands). Among the final-state topologies, only the LEP combined four-jet channel is sufficiently powerful to do so.

²For a Higgs mass of 115.6 GeV, the outcome would follow closely the dotted curve, slightly displaced, so that its minimum coincides with the signal+background expectation (dash-dotted curve) at $m_H = 115.6$ GeV.

2.3 Contributions from single events

The likelihood ratio $-2 \ln Q$ is built up from individual event weights $\ln(1 + s/b)$. The 20 candidates with the highest weights at $m_H = 115$ GeV are listed in Table 3. Some of these candidates are discussed in detail in Ref's [15], [14], [17], [18] and [23]. For the events of

	Expt	E_{cm}	Decay channel	M_H^{rec} (GeV)	$\ln(1 + s/b)$ @115 GeV
1	Aleph	206.7	4-jet	114.3	1.73
2	Aleph	206.7	4-jet	112.9	1.21
3	Aleph	206.5	4-jet	110.0	0.64
4	L3	206.4	E-miss	115.0	0.53
5	Opal	206.6	4-jet	110.7	0.53
6	Delphi	206.7	4-jet	114.3	0.49
7	Aleph	205.0	Lept	118.1	0.47
8	Aleph	208.1	Tau	115.4	0.41
9	Aleph	206.5	4-jet	114.5	0.40
10	Opal	205.4	4-jet	112.6	0.40
11	Delphi	206.7	4-jet	97.2	0.36
12	L3	206.4	4-jet	108.3	0.31
13	Aleph	206.5	4-jet	114.4	0.27
14	Aleph	207.6	4-jet	103.0	0.26
15	Opal	205.4	E-miss	104.0	0.25
16	Aleph	206.5	4-jet	110.2	0.22
17	L3	206.4	E-miss	110.1	0.21
18	Opal	206.4	E-miss	112.1	0.20
19	Delphi	206.7	4-jet	110.1	0.20
20	L3	206.4	E-miss	110.1	0.18

Table 3: Properties of the 20 candidates contributing with the highest weight $\ln(1 + s/b)$ to $-2 \ln Q$ at $m_H = 115$ GeV. The experiment, c.m. energy, decay channel, the reconstructed mass and the weight at $m_H = 115$ GeV are listed. This list is obtained requiring $s/b > 0.2$ or $\ln(1 + s/b) > 0.18$ at $m_H = 115$ GeV. The corresponding expected signal and background rates are 8.8 and 16.5 events, respectively.

each experiment with the highest weight at $m_H = 115$ GeV, the evolution of $\ln(1 + s/b)$ with test-mass is shown in Figure 4. Due to the experimental resolution, candidate events with a given reconstructed mass are seen to have sizeable weights for a range of test-masses, with the maximum weight being for test-masses close to the reconstructed mass.

The distribution of event weights for the test-mass fixed at $m_H = 115.6$ GeV is shown in the upper part of Figure 5 ($\log_{10} s/b$ is plotted for better visibility). For the purpose of this figure, a cut at $s/b > 0.01$ has been introduced. The upper right plot shows the integrals of these distributions, starting from high values of s/b (note that the bins are correlated). The data prefer slightly the signal+background hypothesis over the background hypothesis although

the separation is weak. The two plots in the lower part show the corresponding distributions for a test-mass chosen arbitrarily at $m_H = 110$ GeV. The data show clear preference for the background hypothesis in this case.

There is a general agreement between the observed and simulated rates, see Table 4.

m_H	$\ln(1 + s/b)_{min}$	Expected signal	Expected backgd.	Data
110 GeV	0.01	75.7	440.0	430
	0.1	63.2	128.7	151
	0.18	55.8	77.6	84
	0.5	36.8	22.6	24
	1	21.0	7.0	7
	2	2.5	0.3	1
115 GeV	0.01	17.7	226.5	242
	0.1	11.4	34.8	47
	0.18	8.8	16.5	20
	0.5	4.4	3.4	5
	1	1.6	0.6	2
	2	0.1	0.01	0
115.6 GeV	0.01	13.4	211.7	227
	0.1	7.7	26.2	38
	0.18	5.8	12.4	15
	0.5	2.4	2.0	4
	1	0.8	0.3	1
	2	0.03	0.004	0

Table 4: Expected signal rates (for a SM Higgs boson with a mass of 110, 115, and 115.6 GeV) and background rates, and the observed event count, for various cuts in $\ln(1 + s/b)$.

2.4 Distributions of the reconstructed Higgs boson mass

The reconstructed Higgs boson mass m_H^{rec} is just one of several discriminating variables contributing to the separation of the signal and the background processes and the construction of the likelihood ratio Q . Since in some channels the event selection depends explicitly on the test-mass, the reconstructed mass distributions resulting from the standard combination procedure are biased. The distributions shown in Figure 6 are therefore obtained from special selections where the cuts are applied on quantities (e.g. b-tag variables) which introduce little bias into the m_H^{rec} distribution. Three such selections are shown, with increasing signal purity. In the loose/medium/tight selections the cuts are adjusted in each decay channel to obtain for $m_H = 115$ GeV a signal over background ratio ³ of 0.5/1/2 in the reconstructed mass region

³The signal-to background ratio used in these selection is different from the ratio s/b describing event weights.

above 109 GeV. These spectra are shown merely to illustrate the agreement between the data and the simulation in this important discriminating variable, and should not be used to draw conclusions regarding the significance of a possible signal. Most importantly, it is not claimed that the slight excess at high mass in the tight selection (4 events for an expected background of 1.25 events) is solely responsible for the result quoted below.

2.5 Confidence level calculation

The expected distributions of $-2 \ln Q$ for a test-mass of 115.6 GeV (a slice of Figure 1 at $m_H = 115.6$ GeV) are shown in Figure 7. The distributions for the background and the signal+background hypotheses are normalized and represent probability density functions. The vertical line indicating the observed value lies within the distribution for the signal+background hypothesis. The integral of the background distribution from $-\infty$ to the observed value, $1 - CL_b$, measures the compatibility of the observation with the background hypothesis. Given a large number of background experiments, it is the probability to obtain an event configuration more signal-like than the one observed. Similarly, the integral from $+\infty$ to the observed value of the signal+background distribution, CL_{s+b} , is a measure of compatibility with the signal+background hypothesis.

Calculating $1 - CL_b$ for test-masses between 100 and 120 GeV, Figure 8 is obtained. At $m_H = 115.6$ GeV, where the $-2 \ln Q$ has its minimum (see Figure 1), one gets $1 - CL_b = 0.034$, which corresponds to about two standard deviations⁴. Values of $1 - CL_b$ and CL_s corresponding to $m_H = 115.6$ GeV are listed in Table 5.

It should be noted that these probabilities refer to *local* fluctuations of the background. To obtain the probability for such a fluctuation to appear anywhere within a given mass range of interest, a multiplicative factor has to be applied which is approximated by the width of the mass range divided by the mass resolution. In the present case the range of interest is limited from below by previous exclusion limits (107.9 GeV [9]) and from above by the kinematic limit of the production process $e^+e^- \rightarrow HZ$ (about 116 GeV). The mass resolution averaged over the final-state topologies and experiments is about 3.5 GeV.

⁴For the conversion of $1 - CL_b$ into standard deviations (σ), we adopt a gaussian approximation [24] and use a “one-sided” convention where $1 - CL_b = 2.7 \times 10^{-3}$ would indicate a 3σ “evidence” and $1 - CL_b = 5.7 \times 10^{-7}$ a 5σ “discovery”. The median expectation for pure background is 0.5. Values smaller or larger than 0.5 indicate an excess or deficit, respectively. In this scheme, the current result, $1 - CL_b = 0.034$, corresponds to 2.1σ . The earlier LEP results quoted in the first and second line of Table 1 correspond to 2.2σ and 2.9σ , respectively. This convention is also used in Figure 8 to indicate the levels of significance on the right-hand scale. The ± 1 and ± 2 standard deviation “bands” which show up e.g. in the $-2 \ln Q$ plots correspond to a slightly different, “two-sided”, convention.

	$1 - CL_b$	CL_{s+b}
ALEPH	2.0×10^{-3}	0.94
DELPHI	0.87	0.02
L3	0.24	0.47
OPAL	0.22	0.47
DLO	0.49	0.07
ALO	3.7×10^{-3}	0.83
Four-jet	0.016	0.74
Missing energy	0.40	0.26
All but four-jet	0.34	0.19
LEP	0.034	0.44

Table 5: The background probability $1 - CL_b$ and the signal+background probability CL_{s+b} at $m_H = 115.6$ GeV, for subsets and for all LEP data. DLO/ALO designate subset where the ALEPH/DELPHI data are left out of the combination.

2.6 Bounds for the Higgs boson mass and coupling

The ratio $CL_s = CL_{s+b}/CL_b$ as a function of the test-mass, shown in Figure 9, is used to derive a lower bound for the SM Higgs boson mass ([9], Appendix A). The test-mass corresponding to $CL_s = 0.05$ defines the lower bound at the 95% confidence level. The expected and observed

	Expected limit (GeV)	Observed limit (GeV)
ALEPH	113.8	111.5
DELPHI	113.5	114.3
L3	112.7	112.2
OPAL	112.6	109.4
DLO	114.9	114.8
LEP	115.4	114.1

Table 6: Expected (median) and observed 95% CL lower bounds on the SM Higgs boson mass, for the individual experiments, for DLO (with ALEPH left out of the combination) and for all LEP data combined.

lower bounds obtained for the SM Higgs boson mass are listed in Table 6. The current lower bound from LEP is 114.1 GeV at the 95% confidence level.

The LEP data are used also to set 95% CL upper bounds on the square of the HZZ coupling in non-standard models which assume the same Higgs decay properties as in the SM but where the HZZ coupling may be different. Figure 10 shows the upper bound on $\xi^2 = (g_{HZZ}/g_{HZZ}^{SM})^2$, the square of the ratio of the coupling in such a model to the SM coupling, as a function of the

Higgs boson mass. In deriving this limit, the data collected at $E_{cm} = 161, 172$ and 183 GeV were also included.

3 Cross-checks, uncertainties

(i) It is legitimate to ask whether the excess at 115 GeV mass could be induced by an inadequate treatment of the data close to the kinematic limit of the process $e^+e^- \rightarrow HZ$. To test this hypothesis, the $-2 \ln Q$ curves (the equivalents to Figure 1) have been produced separately for data of different c.m. energies, see Figure 11. In each plot, the vertical line indicates the test-mass $m_H = E_{cm} - M_Z$ GeV, just at the kinematic limit.

In the 189 GeV data, an excess at $m = 97$ GeV has indeed been observed [25] (see the large negative value of $-2 \ln Q$ close to the signal+background prediction) which was due mainly to small excesses in ALEPH and OPAL data compatible with $e^+e^- \rightarrow ZZ$, the dominant background in the vicinity of that mass. This excess still has a significance of about two standard deviations when LEP data from all energies are combined, and one cannot exclude a physics interpretation beyond the SM (e.g. MSSM with several neutral Higgs bosons). However, there is no evidence for a systematic effect at threshold in the data collected at the other energies below 206 GeV.

(ii) The LEP experiments claim systematic errors of typically 5% for their signal estimates and 10% for their background estimates. Most of the errors are estimated from calibration data (e.g. data taken at $E_{cm} = M_Z$ to calibrate the b-tagging performance or to determine the level of non-b background) or from measurements of the e^+e^- annihilations into fermion pairs, WW and ZZ processes. The current implementation of systematic uncertainties (see Ref's [15]-[18] for details) treats errors from the same source as fully correlated between experiments and errors from different sources as uncorrelated. Furthermore, all bins within the same channel have the same errors, and these errors are assumed to have Gaussian distributions. Several tests have been performed to assess the possible impact of this simplified treatment on the result.

(a) If the systematic errors are ignored, $1 - CL_b$ decreases from 3.4% to 3.2%.

(b) The backgrounds in all channels have to be increased coherently by 13% to reduce the excess at 115.6 GeV to the level of one standard deviation, and by 26% to get a typical background result ($1 - CL_b = 0.5$). Such large coherent changes are not consistent with the quoted error estimates.

(c) In a test, the value of $1 - CL_b$ for the observed data was recomputed 1000 times, each time with a set of signal and background estimations chosen randomly according to the assigned systematic uncertainties and their correlations. The distribution of $1 - CL_b$ at $m_H = 115.6$ GeV is shown in Figure 12. From the r.m.s. width of the distribution (about 50% of the mean value) and its asymmetry, one can conclude that the spread of results one can obtain by varying

the signal and background levels according to their errors is of approximately ± 0.2 standard deviations, when $1 - CL_b$ is interpreted in terms of standard deviations. The systematic errors are already incorporated into the quoted result, and this information is provided to demonstrate the limited sensitivity to the quoted systematic effects.

These tests do not address the question of completeness of the systematic errors provided by the experiments for the combination. Since only one of the experimental collaborations has published its final results, changes to the systematic errors provided by the other experiments cannot be excluded.

(iii) A technical uncertainty is ascribed to various approximations which are necessary to speed up the computations. This uncertainty is estimated by comparing the results from different software packages and by reproducing the $-2 \ln Q$, $1 - CL_b$ and CL_s results of individual experiments prior to the combination. For the present paper, the value of $1 - CL_b$ in the vicinity of $m_H = 115.6$ GeV has been determined independently by four combiners; they fall within a range of $\pm 5\%$ (relative). The highest value, $1 - CL_b = 0.034$, is retained as the result.

4 Internal consistency

The excess at $m_H = 115.6$ GeV has been examined in subsets obtained by dividing the data by experiment and by decay channel. It has also been analysed as a function of signal purity.

The first two subdivisions have been addressed in Figures 2 and 3 and Table 5. The corresponding probability density distributions for $m_H = 115.6$ GeV are shown in Figure 13. The largest difference occurs between the subsets of ALEPH and DELPHI. Looking separately at the final state topologies, the excess is mainly concentrating in the four-jet channel. Combining the four experiments while leaving out the four-jet channel, the lowest plot in Figure 13 is obtained.

As seen in Figure 5, the presence of a Higgs boson should affect a substantial part of the event weight distribution. If the data set is subdivided in high- and low-purity subsets by selecting $s/b > 1$ and $s/b < 1$, at which point the two subsamples have approximately equal expected sensitivity, the contributions to $-2 \ln Q$ are consistent, and slightly more signal-like (negative) in the low-purity subset. Hence, the observed excess is not due to a few events with exceptionally high weights only, but is reflected by the whole distribution of event weights.

5 Conclusion

Combining the data from the four LEP experiments, a new lower bound for the mass of the Standard Model Higgs boson has been derived, which is 114.1 GeV at the 95% confidence level. There is an excess which can be interpreted as production of a Standard Model Higgs boson

with a mass higher than the quoted limit. It is concentrated mainly in the data sets with centre-of-mass energies higher than 206 GeV. The likelihood test designates 115.6 GeV as the preferred mass. The probability for a fluctuation of the Standard Model background is 3.4%. This effect is mainly driven by the ALEPH data and the four-jet final state.

THE RESULTS QUOTED IN THIS PAPER ARE NOT FINAL
SINCE THEY COMBINE PRELIMINARY RESULTS FROM THREE EXPERIMENTS
WITH FINAL RESULTS FROM ONE EXPERIMENT

ACKNOWLEDGEMENTS

We congratulate our colleagues from the LEP Accelerator Division for the successful running in the year 2000 at the highest energies, and would like to express our thanks to the engineers and technicians in all our institutions for their contributions to the excellent performance of the four LEP experiments. The LEP Higgs working group acknowledges the fruitful cooperation between the experiments in developing the combination procedures and in putting them into application.

References

- [1] P.W. Higgs, Phys. Lett. **12** (1964) 132; Phys. Rev. Lett. **13** (1964) 508; Phys. Rev. **145** (1966) 1156; F. Englert and R. Brout, Phys. Rev. Lett. **13** (1964) 321; G.S. Guralnik, C.R. Hagen, and T.W.B. Kibble, Phys. Rev. Lett. **13** (1964) 585.
- [2] S. Weinberg, Phys. Rev. Lett. **19** (1967) 1264; *Elementary Particle Theory*, A. Salam, ed. N. Svartholm (Almqvist and Wiksell, Stockholm, 1968), 367.
- [3] N. Cabibbo, L. Maiani, G. Parisi and R. Petronzio, Nucl. Phys. **B158** (1979) 295; R. Dashen and H. Neuberger, Phys. Rev. Lett. **50** (1983) 1897.
- [4] M. Lindner, M. Sher and H.W. Zaglauer, Phys. Lett. **228B** (1989) 139; M. Sher, Phys. Lett. **317B** (1993) 159; *ibid.* **331B** (1994) 448; G. Altarelli and I. Isidori, Phys. Lett. **337B** (1994) 141; J.A. Casas, J.R. Espinosa and M. Quirós, Phys. Lett. **342B** (1995) 89.
- [5] T. Hambye and K. Riesselmann, Phys. Rev. **D55** (1997) 7255.
- [6] Y. Okada, M. Yamaguchi, and T. Yanagida, Theor. Phys. **85** (1991) 1; H. Haber and R. Hempfling, Phys. Lett. **66** (1991) 1815; J. Ellis, G. Ridolfi, and F. Zwirner, Phys. Lett. **B257** (1991) 83; R. Barbieri and M. Frigeni, Phys. Lett. **B258** (1991) 395; S. Heinemeyer, W. Hollik and G. Weiglein, Eur. Phys. Jour. **C9** (1999) 343; M. Carena, M. Quirós and C. Wagner, Nucl. Phys. **B461** (1996) 407; H. Haber, R. Hempfling and A. Hoang, Z. Phys. **C75** (1997) 539.
- [7] Ch. Kolda and H. Murayama, *The Higgs Mass and New Physics Scales in the Minimal Standard Model*, hep-ph/0003170 (March 2000).
- [8] The LEP Electroweak Working Group, public page,
<http://lepewwg.web.cern.ch/LEPEWWG/> (updated July 10, 2001).
- [9] ALEPH, DELPHI, L3 and OPAL Collaborations, The LEP working group for Higgs boson searches, *Searches for Higgs bosons: Preliminary combined results using LEP data collected at energies up to 202 GeV*, CERN-EP/2000-055.
- [10] ALEPH, DELPHI, L3 and OPAL Collaborations, The LEP working group for Higgs boson searches, *Searches for Higgs bosons: Preliminary combined results using LEP data collected at energies up to 209 GeV*, ALEPH 2000-074 CONF 2000-051, DELPHI 2000-148 CONF 447, L3 Note 2600, OPAL Technical Note TN661, submitted to ICHEP'2000, Osaka, Japan, July 27-August2, 2000.
- [11] Shan Jin, *Search for Standard Model Higgs Boson at LEP2*, Proc. ICHEP-2000, Ed. C.S. Lim, T. Yamanaka, Vol II, p. 1105; P. Igo-Kemenes, *Searches for New Particles and New Physics: Results from e⁺e⁻ Colliders*, *ibidem*, Vol. I, p. 133.
- [12] D. Schlatter for the ALEPH Collaboration, LEP Committee Open Session, 5.9.2000.
- [13] P. Igo-Kemenes for the LEP Higgs working group, LEP Committee Open Session, 3 November, 2000, <http://lephiggs.web.cern.ch/LEPHIGGS/talks/index.html>.

- [14] L3 Collaboration, M. Acciarri et al., Phys. Lett. **B495** (2000) 18.
- [15] ALEPH Collaboration, R. Barate et al., Phys. Lett. **B495** (2000) 1.
- [16] DELPHI Collaboration, P. Abreu et al., Phys. Lett. **B499** (2001) 23.
- [17] L3 Collaboration, M. Acciarri et al., Phys. Lett. **B**, submitted for publication.
- [18] OPAL Collaboration, G. Abbiendi et al., Phys. Lett. **B499** (2001) 38.
- [19] J. Ellis, M.K. Gaillard, and D.V. Nanopoulos, Nucl. Phys. **B106** (1976) 292;
 B.L. Joffe and V.A. Khoze, Sov. J. Part. Phys. **9** (1978) 50;
 B.W. Lee, C. Quigg and H.B. Thacker, Phys. Rev. **D16** (1977) 1519;
 J.D. Bjorken, Proc. 1976 SLAC Summer Inst. Part. Phys., ed. M.C. Zipf (SLAC report 198, 1977) 1.
 F.A. Behrends and R. Kleiss, Nucl. Phys. **B260** (1985) 32.
- [20] W. Kilian, M. Kramer, and P.M. Zerwas, Phys. Lett. **B373** (1996) 135.
- [21] A.L. Read, *Linear interpolation of histograms*, Nucl. Instr. Methods **A 425** (1999) 357.
- [22] K.S. Cranmer, *Kernel Estimation in High Energy Physics*, Comput. Phys. Commun. **136** (2001) 198.
- [23] L3 Collaboration, *Search for the SM Higgs boson with the L3 experiment at LEP*, L3 Note 2688, June 2001.
- [24] D.E. Groom et al., *Review of particle physics*, Eur. Phys. Journ. **C15** (2000) 1.
- [25] ALEPH, DELPHI, L3 and OPAL Collaborations, and the LEP Higgs Working Group, *Searches for Higgs bosons: Preliminary combined results from the four LEP experiments at $\sqrt{s} \approx 189$ GeV*, ALEPH-CONF 99-052, DELPHI-CONF 327, L3 Note 2442, OPAL TN 6614 (July 1999).

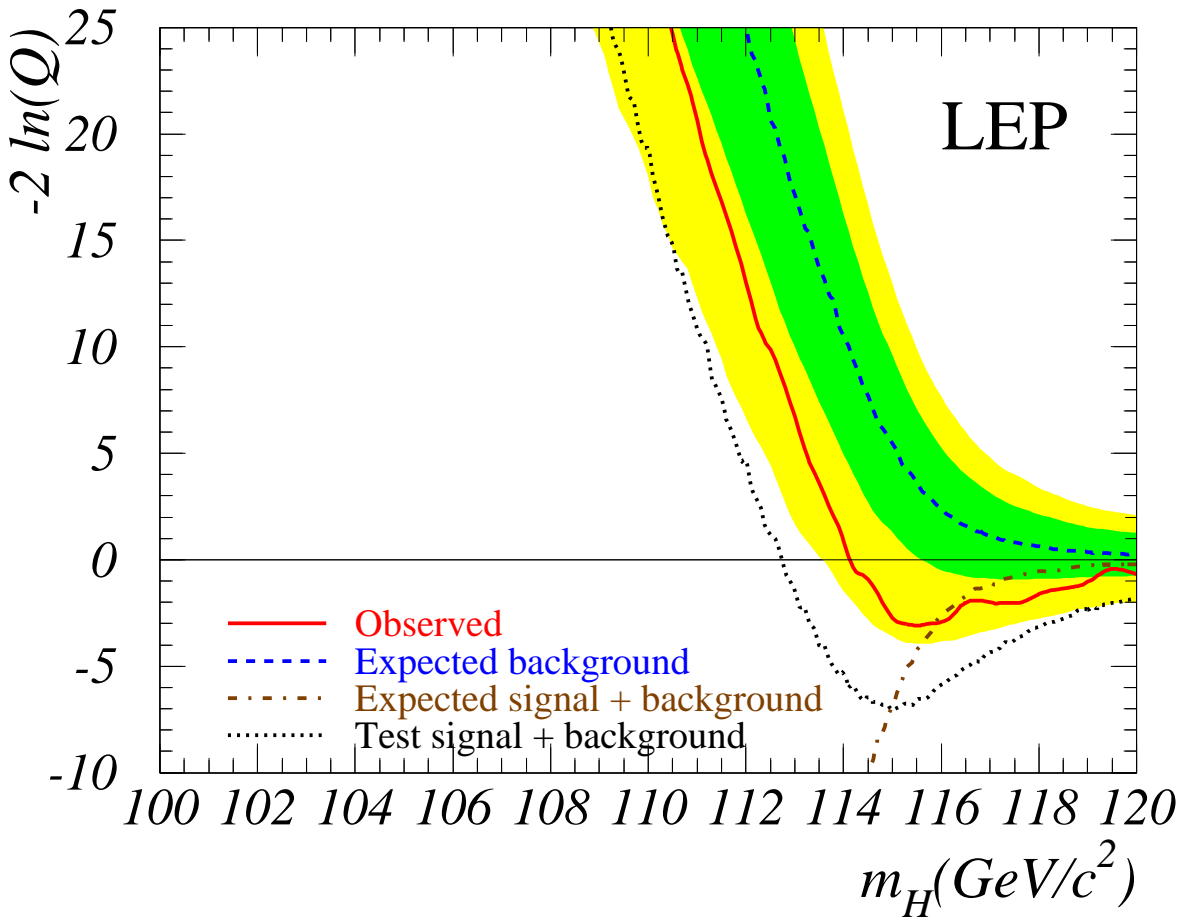


Figure 1: Observed and expected behaviour of the likelihood ratio $-2 \ln Q$ as a function of the test-mass m_H , obtained by combining the data of all four experiments. The solid line represents the observation; the dashed/dash-dotted lines show the median background/signal+background expectations. The dark/light shaded bands around the background expectation represent the $\pm 1/\pm 2$ standard deviation spread of the background expectation obtained from a large number of background experiments. The dotted line is the result of a test where the signal from a 115 GeV Higgs boson has been added to the background and propagated through the likelihood ratio calculation.

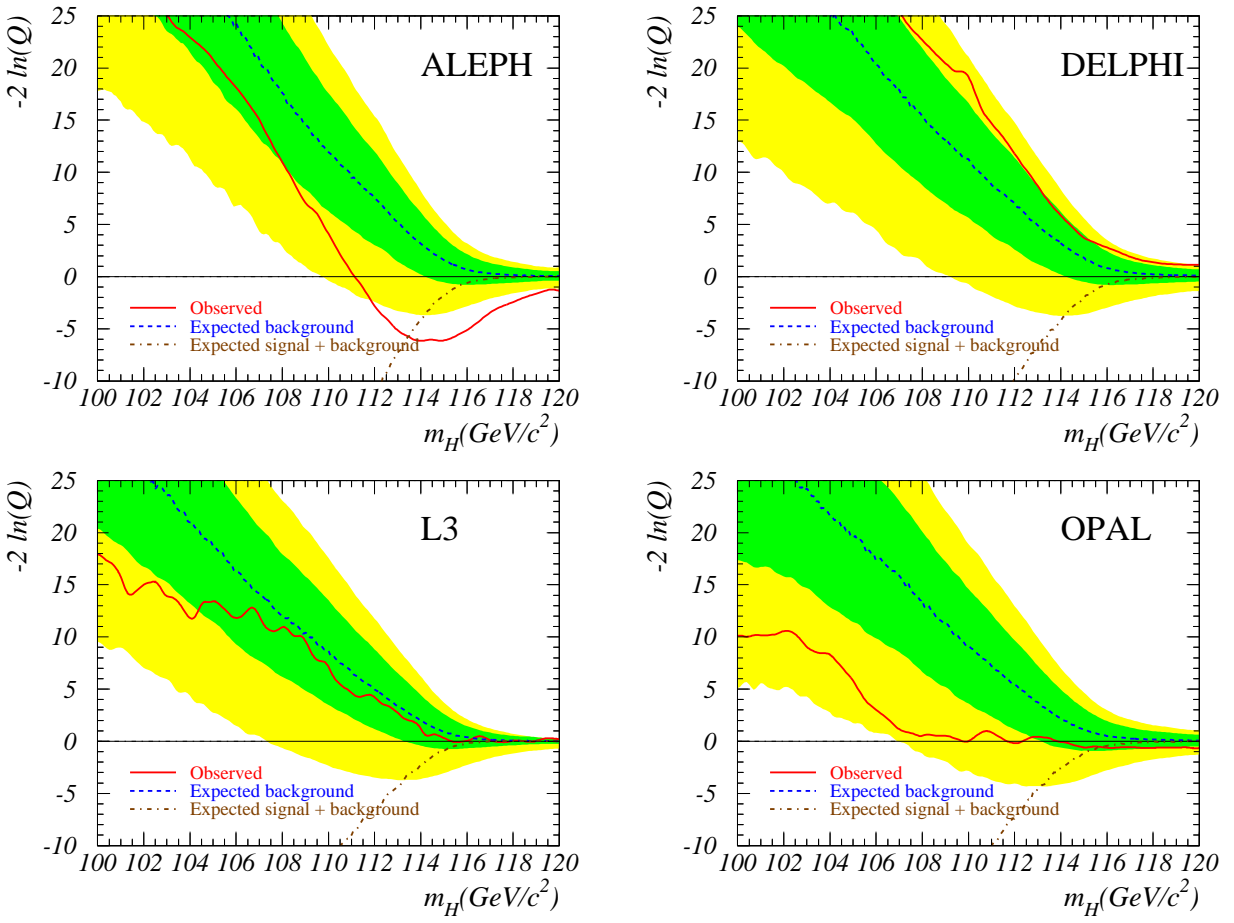


Figure 2: Observed and expected behaviour of the test statistic ($-2 \ln Q$) as a function of the test-mass m_H obtained when the combination procedure is applied to the data sets from single experiments (see Figure 1 for the notations).

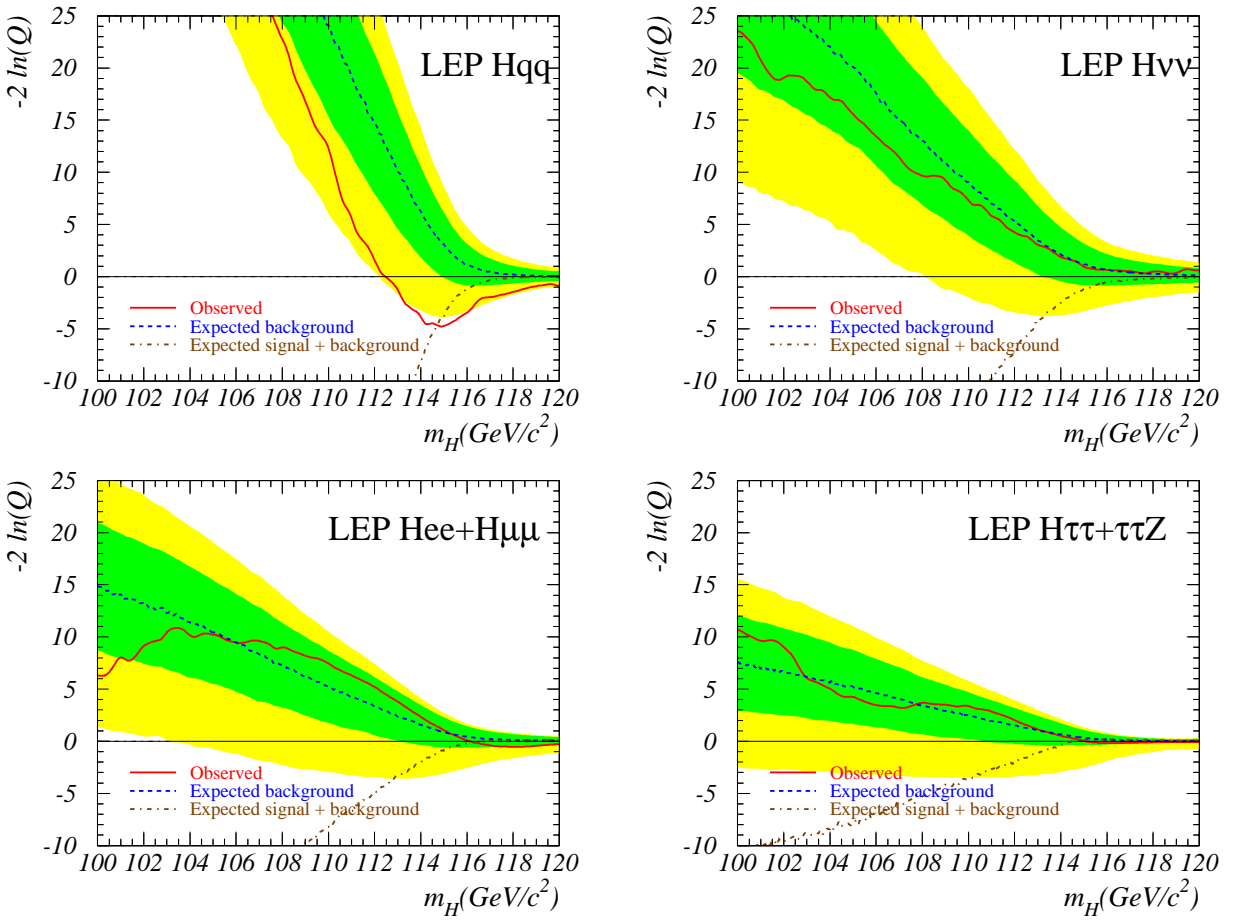


Figure 3: Observed and expected behaviour of the test statistic ($-2 \ln Q$) as a function of the test-mass m_H obtained when the combination procedure is applied to the inputs corresponding to separated decay channels (see Figure 1 for the notations).

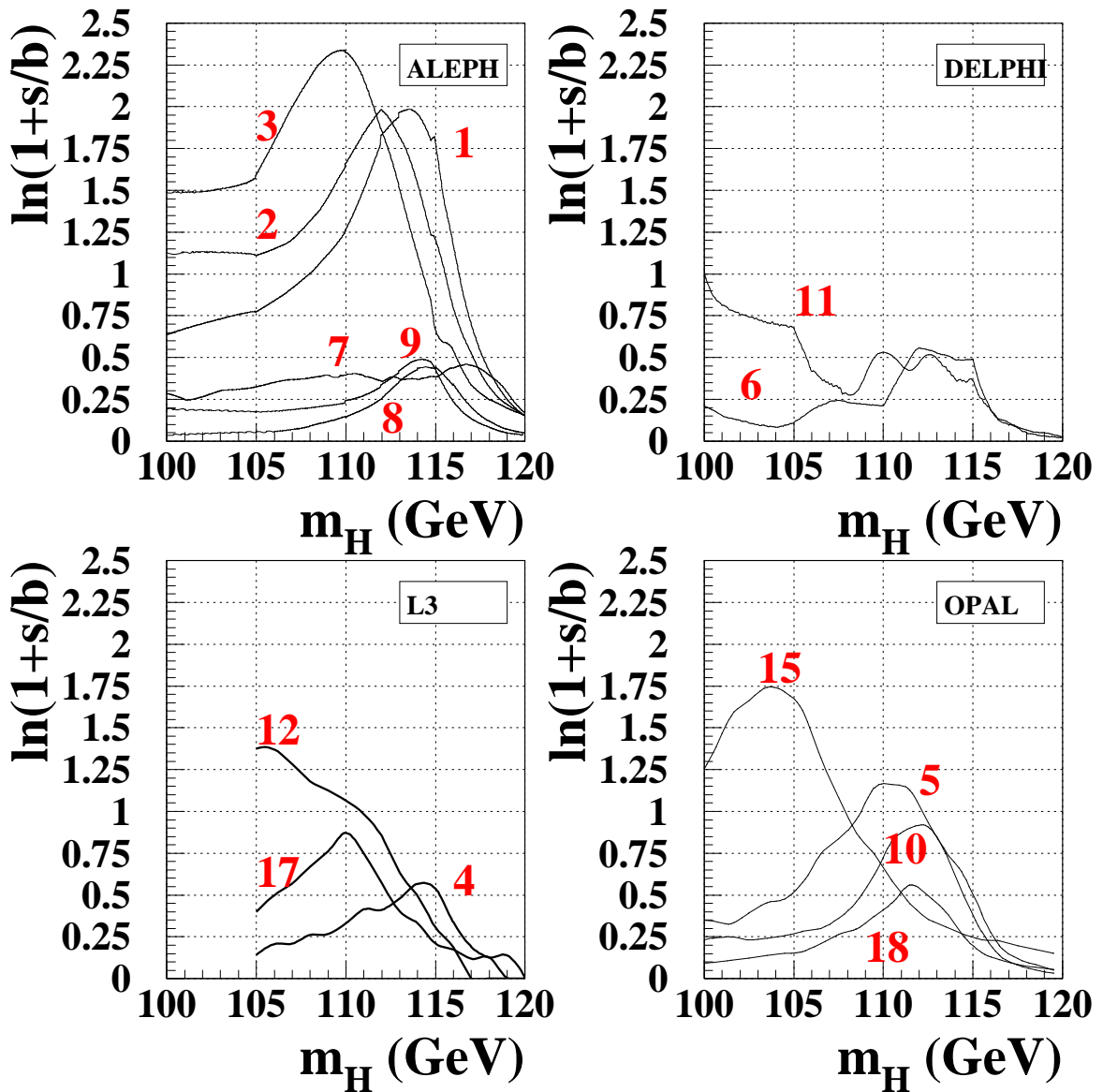


Figure 4: Evolution of the event weight $\ln(1+s/b)$ with test-mass m_H , for the events with the largest contributions to $-2\ln Q$ at $m_H = 115$ GeV. The labels correspond to the numbering in the first column of Table 3.

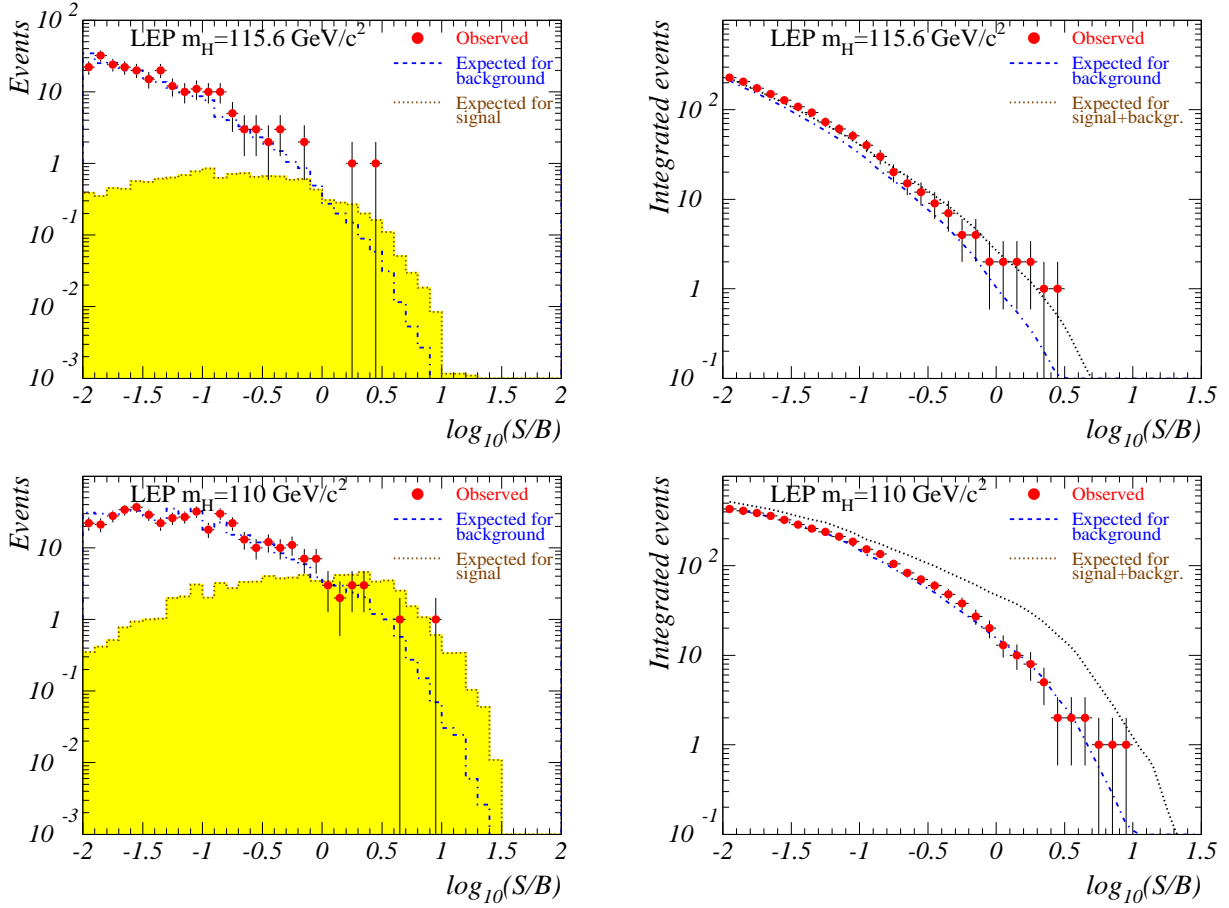


Figure 5: Left hand side: expected and observed distributions of $\log_{10}s/b$ for a test-mass of $m_H = 115.6 \text{ GeV}$ (upper part) and 110 GeV (lower part). White/shaded histograms: expected distributions for the background/signal; points with error bars: selected data. Right hand side: the integrals, from right to left, of the distributions shown in the plots on the left hand side. Dash-dotted/dotted lines: expected for background/signal+background.

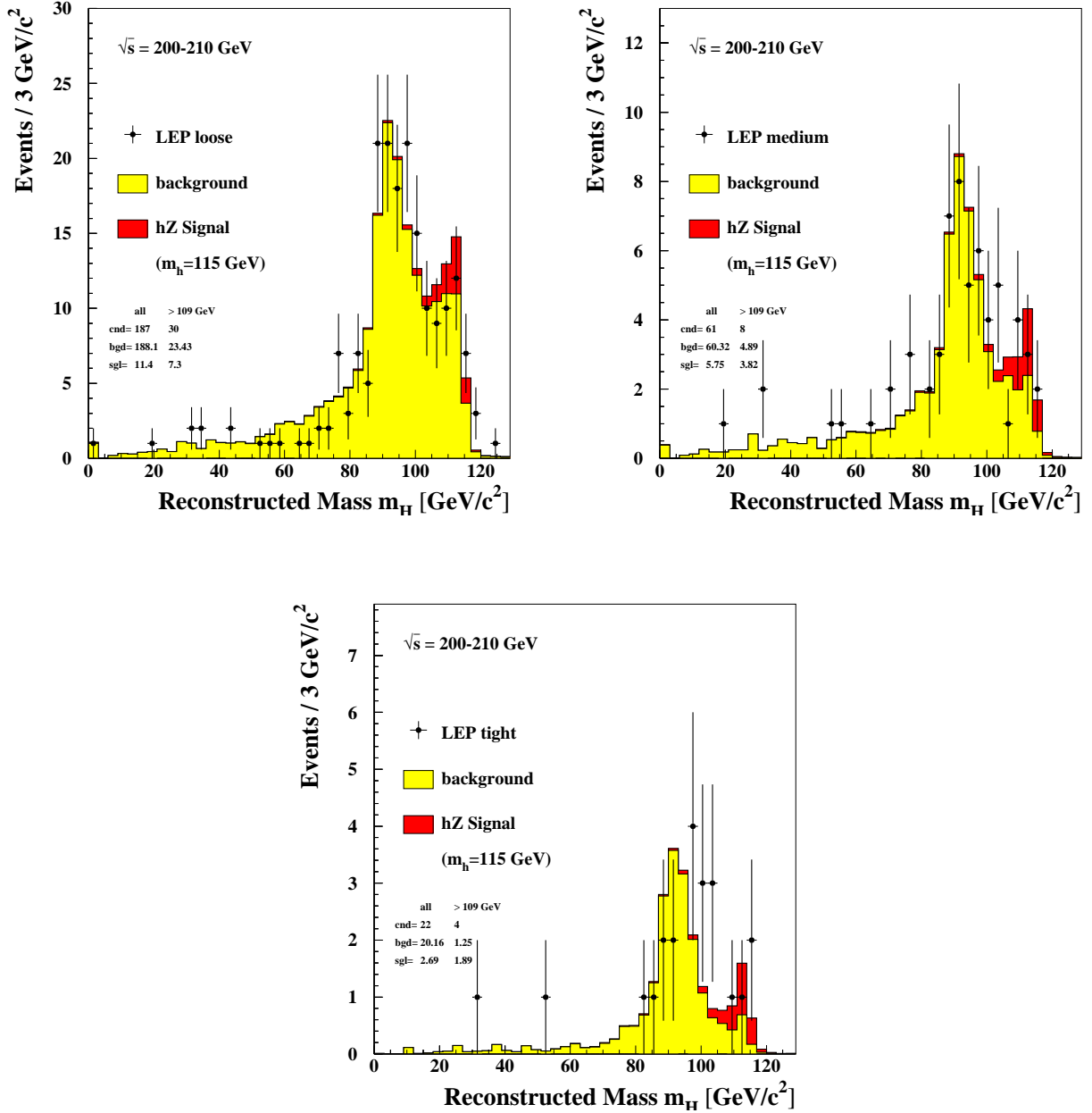


Figure 6: Distributions of the reconstructed Higgs mass, m_H^{rec} , from three special, non-biasing, selections with increasing purity of a signal from a 115 GeV Higgs boson.

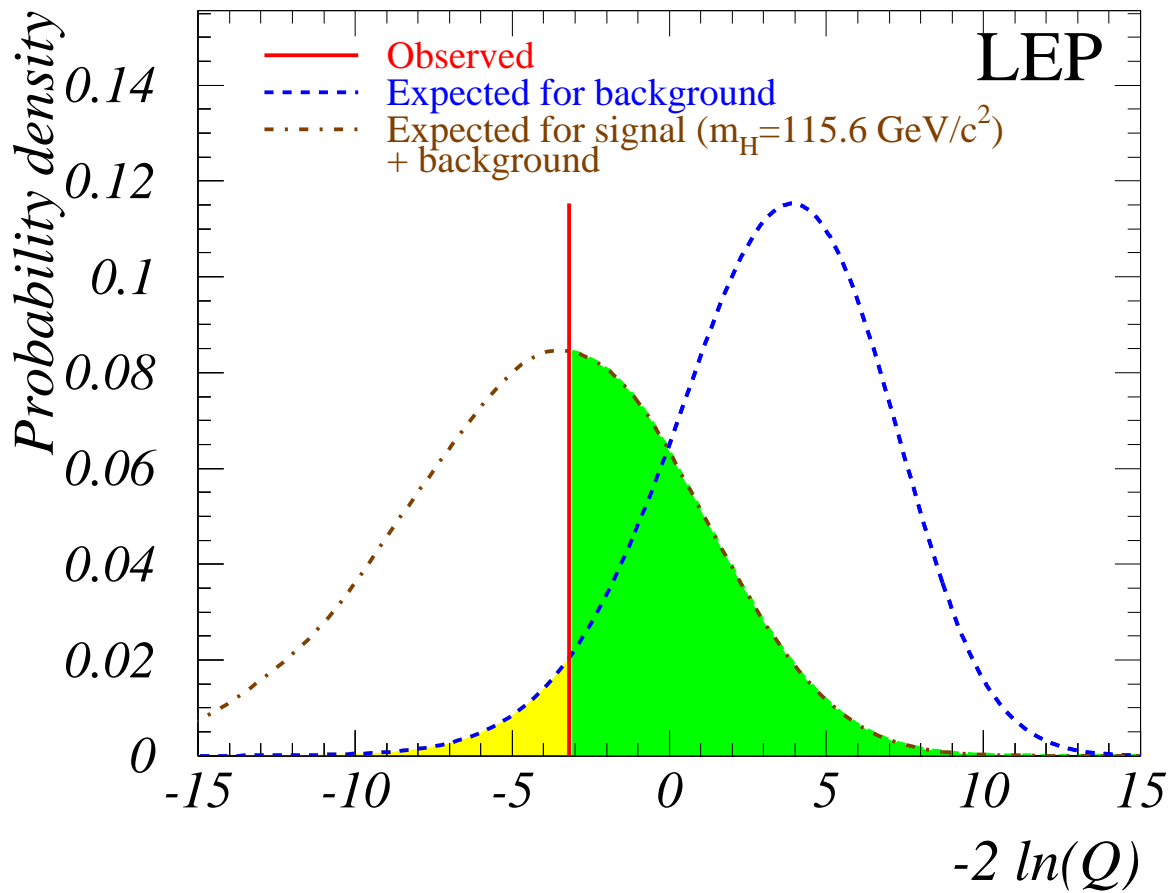


Figure 7: Probability density functions corresponding to a test-mass $m_H = 115.6$ GeV, for the background and signal+background hypotheses. The observed value of $-2 \ln Q$ which corresponds to the data is indicated by the vertical line. The light shaded region is a measure of the compatibility with the background hypothesis, $1 - CL_b$, and the dark shaded region is a measure of compatibility with the signal+background hypothesis, CL_{s+b} .

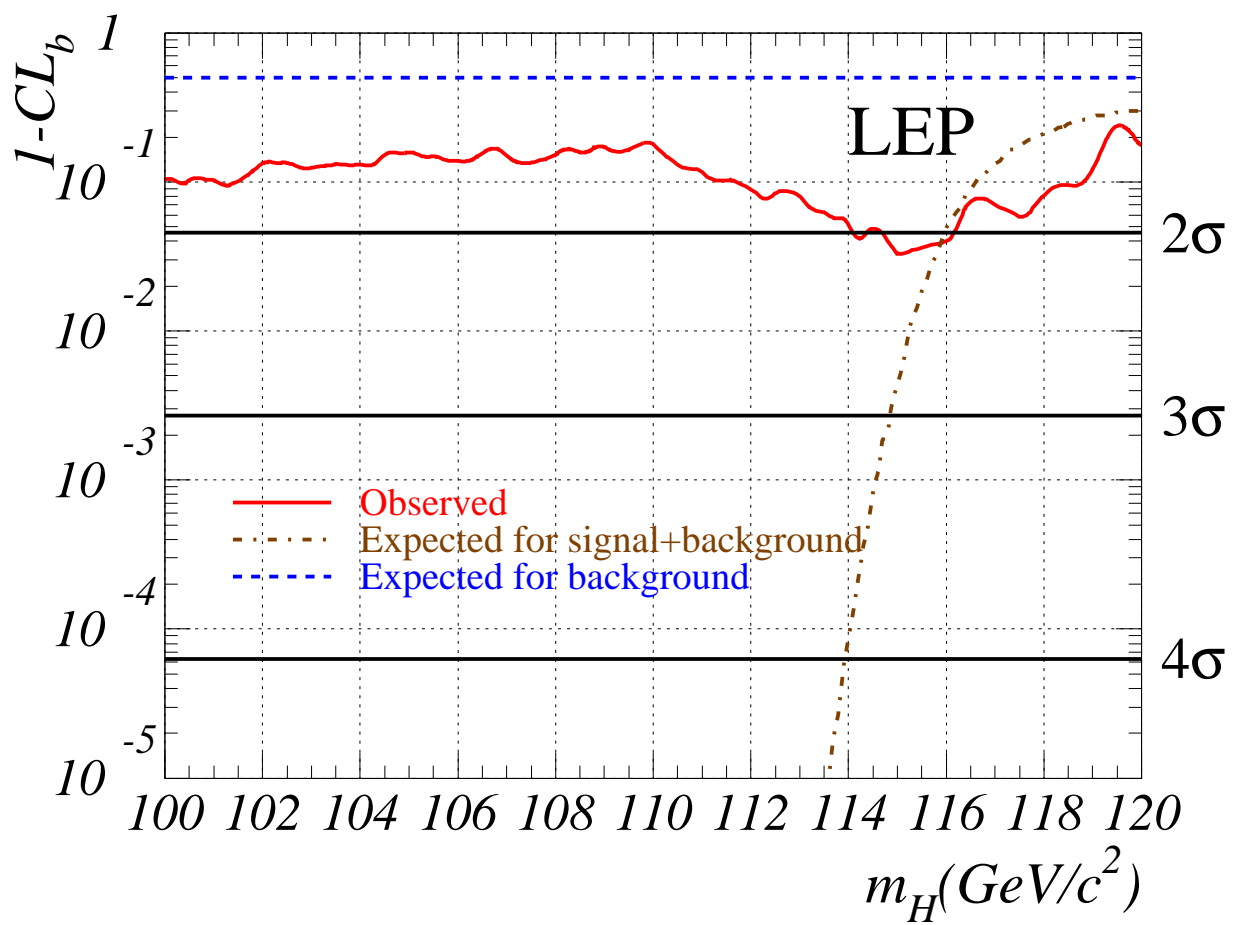


Figure 8: The probability $1 - CL_b$ as a function of the test-mass m_H . Solid line: observation; dashed/dash-dotted lines: expected probability for the background/signal+background hypotheses. See Footnote ⁴ for the transformation of $1 - CL_b$ values into standard deviations.

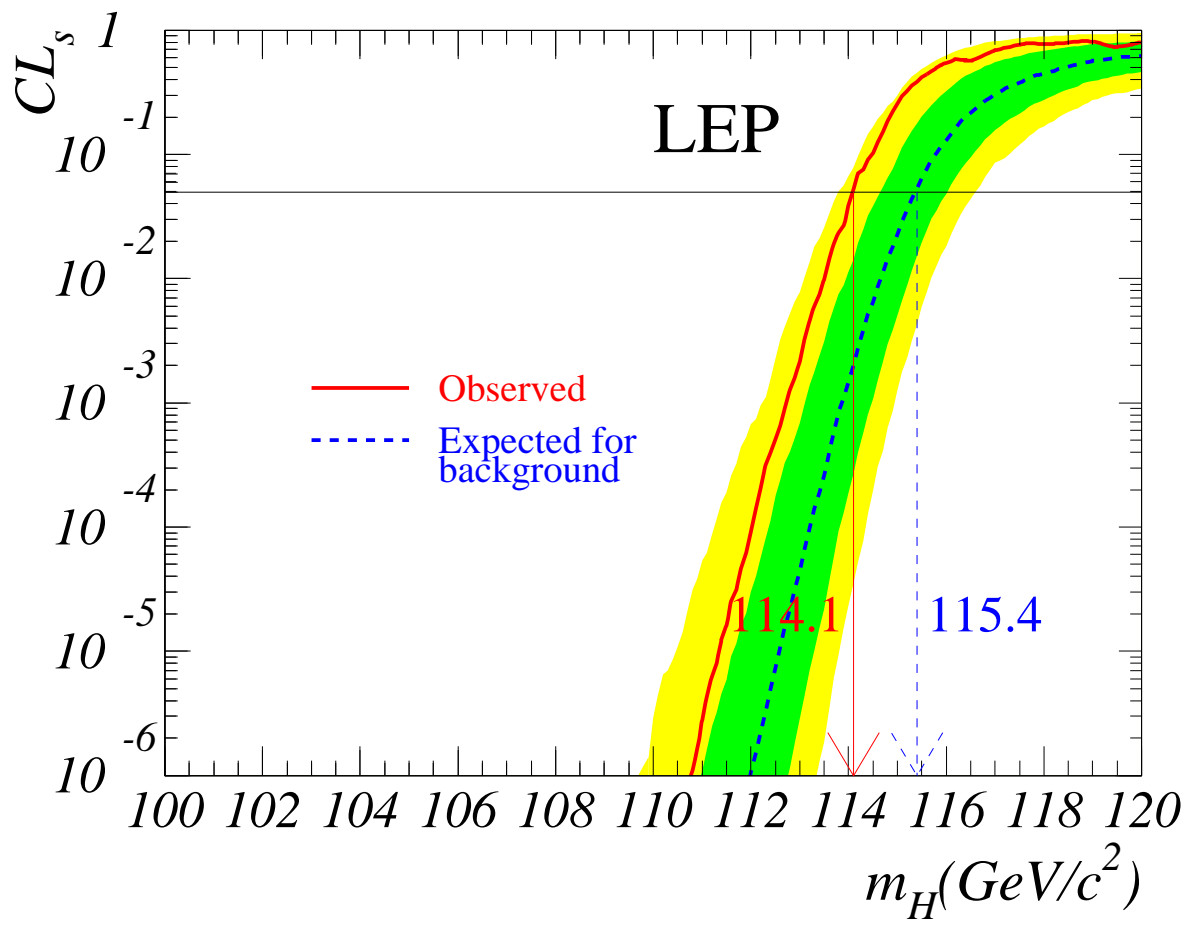


Figure 9: Confidence level CL_s for the signal+background hypothesis. Solid line: observation; dashed line: median background expectation. The dark/light shaded bands around the median expected line correspond to the $\pm 1/\pm 2$ standard deviation spreads from a large number of background experiments.

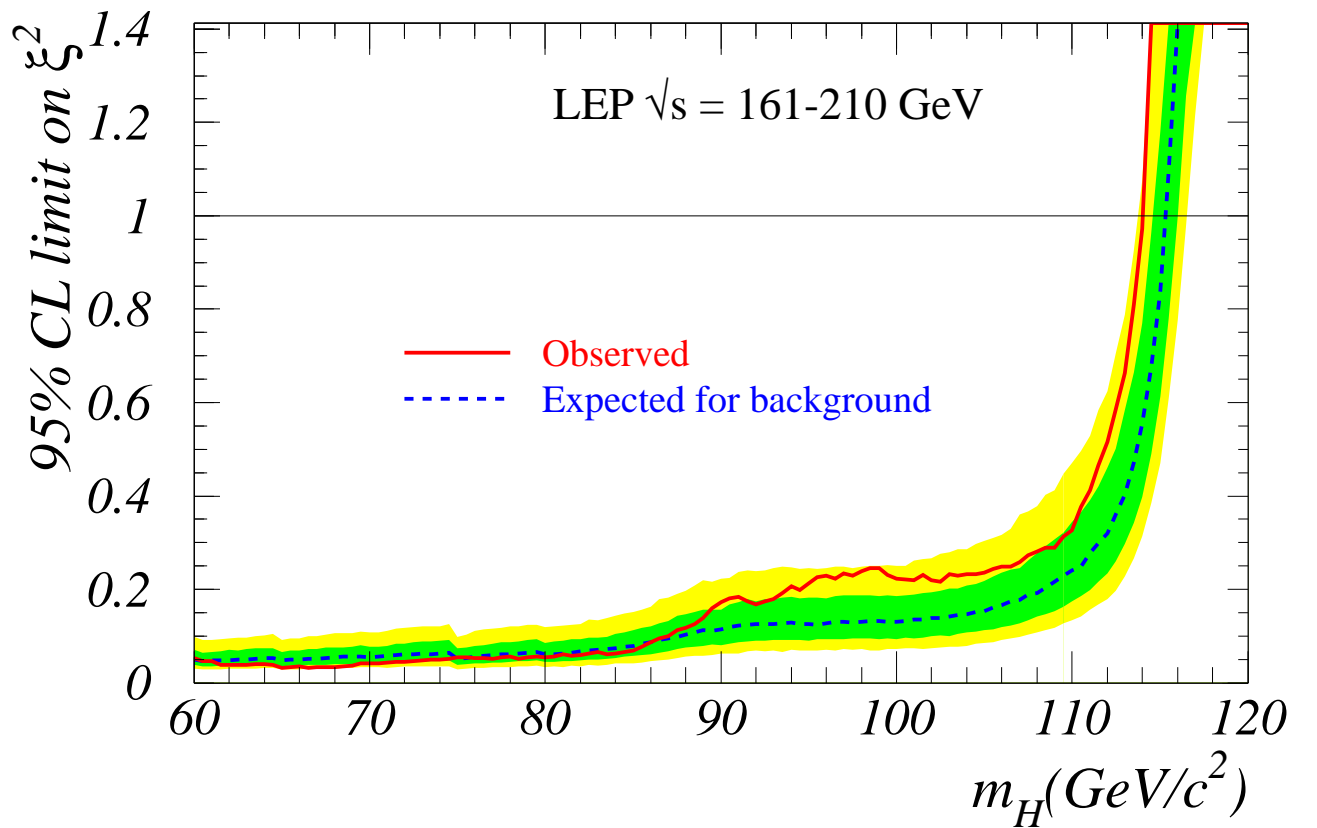


Figure 10: The 95% CL upper bound on ξ^2 as a function of m_H , where $\xi = g_{HZZ}/g_{HZZ}^{SM}$ is the HZZ coupling relative to the SM coupling. The dark/light shaded bands around the median expected line correspond to the $\pm 1/\pm 2$ standard deviation spreads from a large number of background experiments. The horizontal line corresponds to the SM coupling.

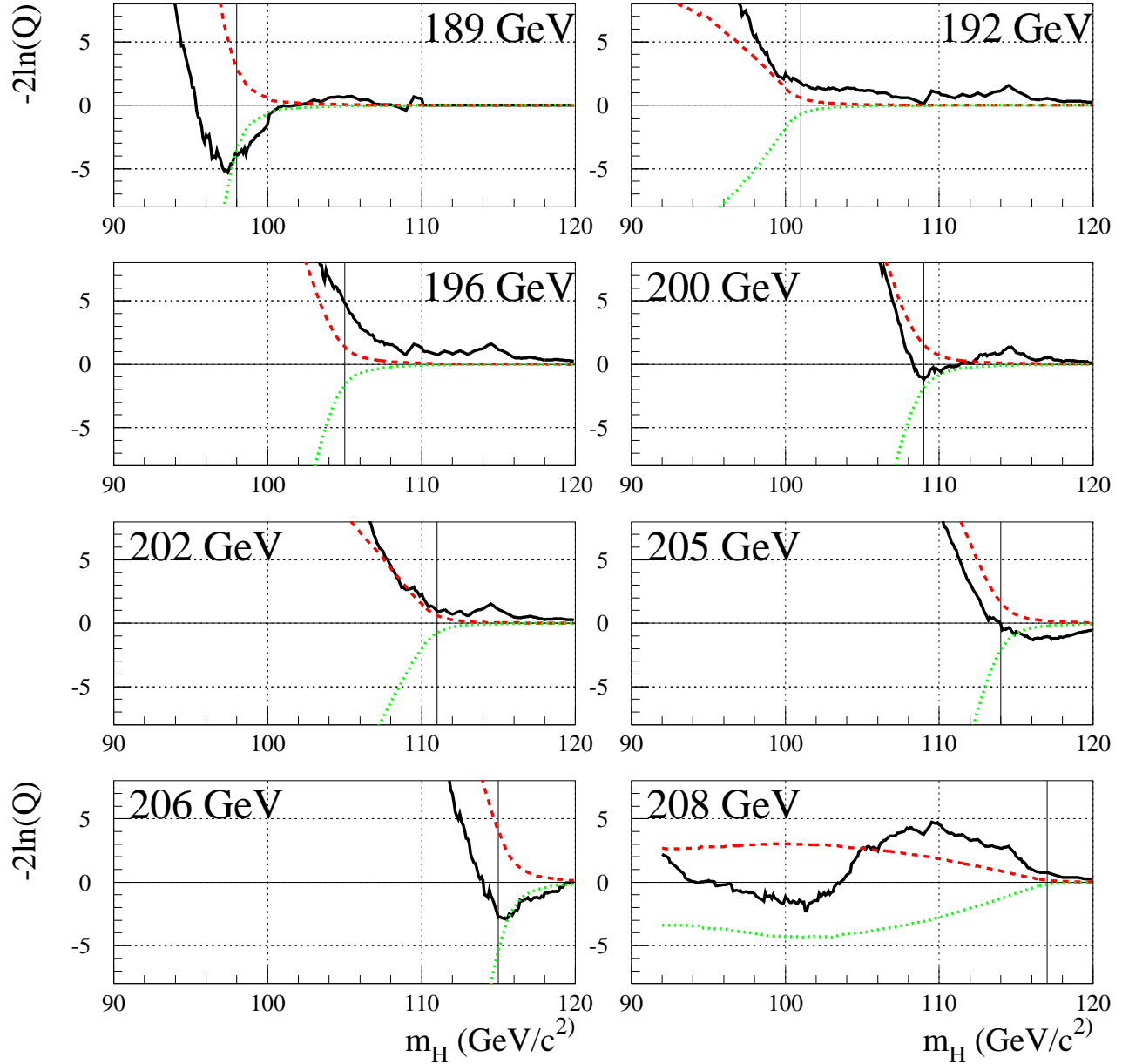


Figure 11: Behaviour of $-2 \ln Q$ in subsets collected at different c.m. energies. In each plot, the full curve shows the observed behaviour, the dashed/dotted lines show the expected behaviour for background/signal+background, and the vertical line indicates the test-mass $m = E_{cm} - M_Z$ GeV, just at the kinematic limit. (The subset labelled 208 GeV has very low statistics.)

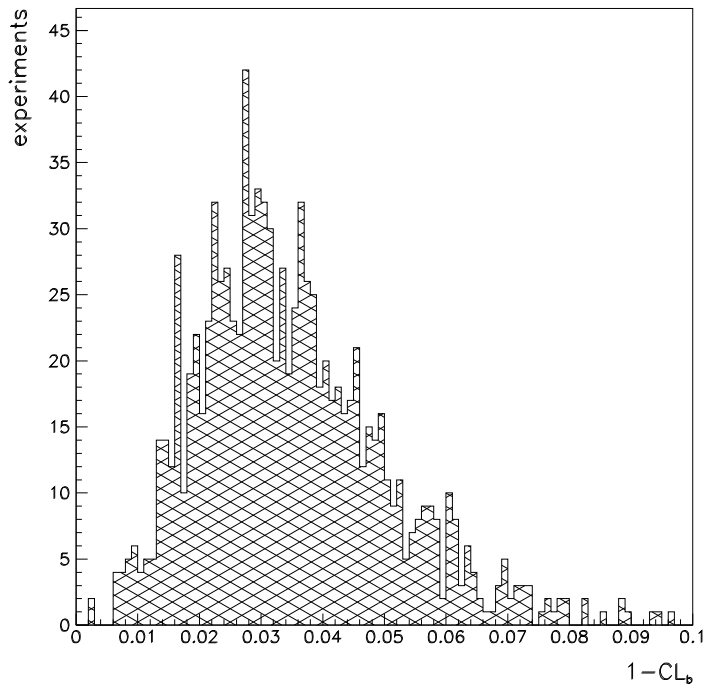


Figure 12: Distribution of the background probability $1 - CL_b$ for a test-mass of 115.6 GeV obtained from 1000 simulated experiments where the expected signal and background has been varied randomly according to the systematic errors and their correlations.

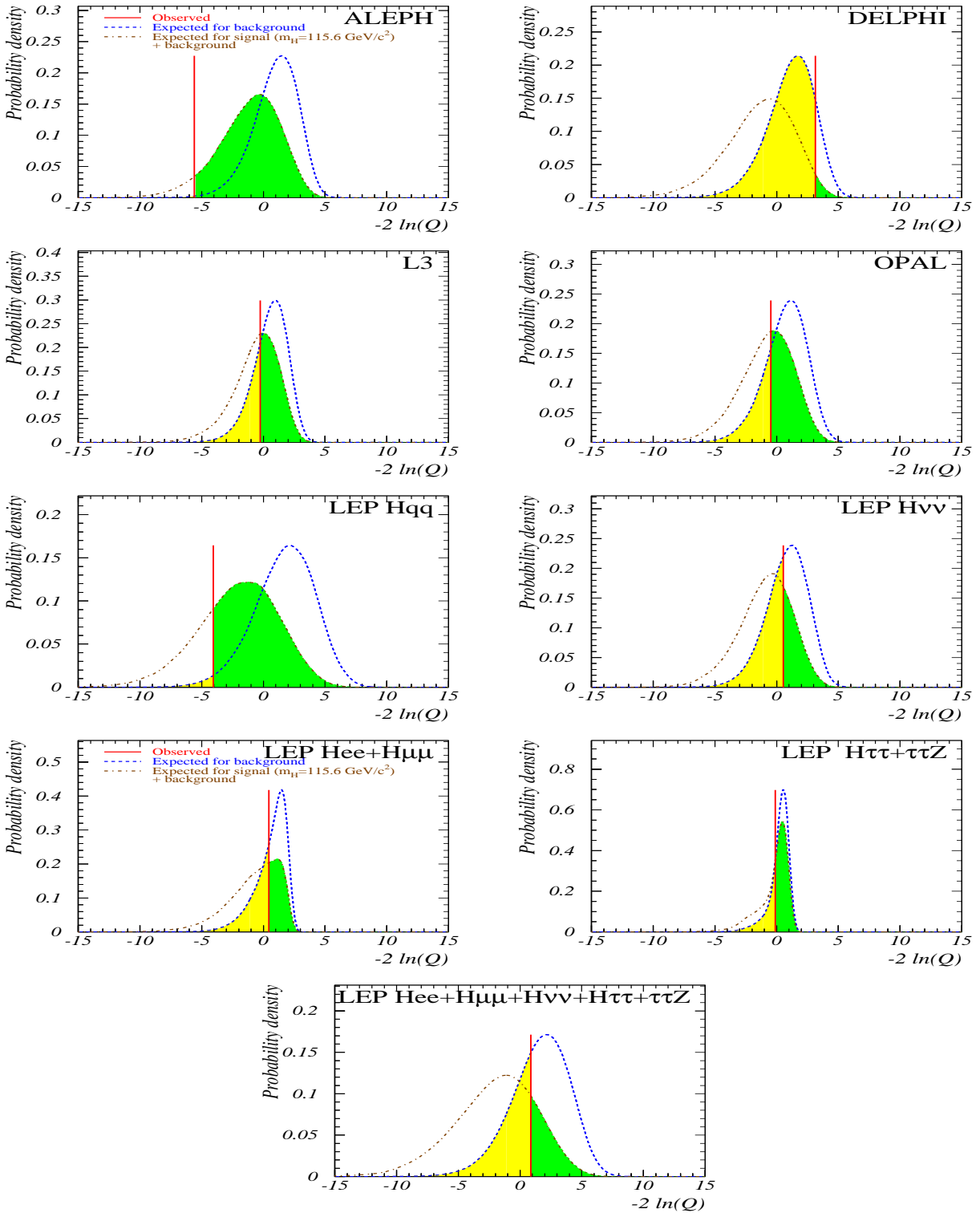


Figure 13: Probability density functions corresponding to a test-mass $m_H = 115.6$ GeV for subsets of the data. Upper four plots: subdivision by experiments; next four plots: subdivision by decay channels. The lowest plot combines all but the four-jet channel. In each case, the observed value of $-2 \ln Q$ is indicated by the vertical line.